MDPI

Article

DLM-LSTM Framework for North-south Land Deformation Trend Analysis from Low Cost GPS Sensor Time Series

Fangling Pu [1,2,†*], Zhaozhuo Xu [1,†], Nengcheng Chen [2,3], and Jianya Gong [2,3],

1 School of Electronic Information, Wuhan University, Wuhan, Hubei 430072, China; flpu@whu.edu.cn; xuzhaozhuo@whu.edu.cn
2 Collaborative Innovation Center of Geospatial Technology, Wuhan University, Wuhan, Hubei 430079; flpu@whu.edu.cn; cnc@whu.edu.cn; gongjy@whu.edu.cn
3 State Key Laboratory for Information Engineering in Surveying, Mapping and Remote Sensing (LIESMARS), Wuhan University, Wuhan, Hubei 430079, China; cnc@whu.edu.cn; gongjy@whu.edu.cn
* Correspondence: flpu@whu.edu.cn; Tel.: +86-18971692061
† These authors contributed equally to this work.

Academic Editor: name
Version August 31, 2017 submitted to Entropy

Abstract: Landslides endanger regular industrial production and human safety. Displacement trend analysis gives an explicit way to observe and forecast landslides. Although satellite borne remote sensing methods such as synthetic aperture radar have gradually substituted manual measurement in detecting deformation trend, they failed to observe displacement in north-south direction. Wireless low cost GPS sensors are developed to assist remote sensing method in north-south deformation monitoring because of their high temporal resolution and widely usage. In our paper, a DLM-LSTM framework is developed to extract and predict north-south land deformation trend from meter accuracy GPS receivers. Dynamic linear model is introduced to model the relation between measurement and the state vector that includes trend, periodic variation and autoregressive factors in discontinuous low cost latitude time series. The deformation trend with centimeter level accuracy is extracted by Kalman filter and smoother. With validated input as prior knowledge, LSTM network shows its power by predicting deformation trend in centimeter level accuracy too. This is the first time that sub-meter level deformation trend is detected from wireless low cost GPS sensors with meter level navigation error. The framework will have a broad application prospects in geological disaster monitoring.

Keywords: Land Deformation; Dynamic Linear Model;Recurrent Neural Networks; Trend Anaylsis.

1. Introduction

Due to long term exploitation, landslides threaten the safety of coal mine workers and nearby residents [1]. Continuous deformation on the surface of coal mine is one of the main incentives for landslides. Most of time, the surface displacement slowly changes or almost steadily versus time [2]. Once the displacement exceeds the maximum tolerance of the land surface, large slope failure becomes unstoppable[3], [4]. Constant deformation monitoring captures necessary information for landslide researches. After summarizing the laws of long time land surface motion, early warnings can be communicated to local people [5].

Time series constructed from globe positioning systems (GPS) observation provide indispensable information about north-south land surface deformation. Compared with large scale observation, such as satellite borne synthetic aperture radar (SAR), GPS receivers have advantage in high time resolution and north-south displacement observation. Although large scale of centimeter

displacements can be observed through processing remote sensing image time series obtained by SAR and differential interferometric SAR (DInSAR) [6] [7], North-south ground motion are difficult to spot. Traditional DInSAR only performs well in observing up-down and east-west displacements [8], [9]. Although a great number of studies have engaged in modifying conventional SAR image processing algorithms [10] to detect north-south deformation, SAR and DInSAR solutions are still too sophisticated to handle it alone. Therefore, in past cases, GPS latitude time series obtained by manual point measurement supplement remote sensing approaches in north-south deformation detection.

With rapid development of Information Communication Technology (ICT), interconnected GPS sensors form wireless sensor networks to substitute manual measurement in long-term, high temporal resolution land deformation monitoring. Spatial distributed autonomous sensor systems save plenty of labor costs and generate massive data streams about the ground truth.

However, time series obtained from wireless GPS sensors suffer in both accuracy and continuity. Real time differential GPS techniques, such as Real-Time Kinematic (RTK) [11], improve positional accuracy through sending corrections from a base station to a RTK terminal in real time. Centimeter or millimeter accuracy of displacement measurements can be obtained with RTK. But the cost of establishing RTK and their operation is high, which hinders popularization and application of RTK. Instead, current wireless GPS sensor networks use low cost GPS receiver that is widely found in smartphones, vehicles and unmanned aerial vehicles (UAV). This kind of GPS sensor usually receives satellite C/A (Coarse Acquisition) codes on the L1 frequency (1.57542 GHz). The coordinates that are read from a low cost GPS receiver will be within 3 to 15 meters of the true position on the earth, which exhibit significant errors in positioning. Meanwhile, because most wireless GPS sensors are deployed at rural areas, unstable power supply becomes inevitable. Limited energy leads to GPS sensor dysfunction, which generates discontinuous points in latitude time series. In current stage, problems in both sensor materials and power supply cannot be solved immediately. The full use of low cost, discontinuous GPS latitude stream requires advanced processing paradigm.

Any observed time series can be decomposed into three components: trend, seasonal variation and unsystematic irregular fluctuations. For noisy fragmented time series, trend expresses the dynamic movement in most explicit way, and thus, we put trend analysis as our overriding tasks in low cost GPS land deformation monitoring. Recently, methods proposed to trend analysis can be summarized as two step procedures, which is trend extraction and prediction. The unprocessed, raw time series is firstly smoothed to filter noises and seasonal variations with the aim of obtaining validated trends. Then the extracted trends are used as training samples to get estimations about future values.

There is a wealth of literature concerning the trend extraction and prediction of low cost GPS time series[12]. However, a comprehensive trend analysis framework still remains to be undeveloped. For trend extraction jobs, researchers at first utilized Kalman filters[13] for precision improvement to get trends with high accuracy. Although Kalman filter has good performance in denoising Gaussian noise, the simplicity of Kalman state space function limits its power in filtering out complex periodical variations. Based on this situation, empirical mode decomposition (EMD) is introduced in paper[14], [15] to complement Kalman filter in non-linear and non-Gaussian fluctuation removal. But the unexplained intrinsic mode functions (IMF) generated during EMD sifting makes it less reliable. Also experiments in Early Warning of Abrupt Displacement Change at the Yemaomian Landslide of the Three Gorge Region, China[16] shows displacement fluctuations can be detected by autoregressive model (AR), which is not considered in previous Kalman or EMD approaches. Thus, an unified model that combines spline smoothing, periodical variation detection and AR process estimations is still required. For trends prediction, Recurrent Neural Networks (RNNs), particularly with Long Short-Term Memory (LSTM) hidden units are widely acknowledged as powerful state-of-art prediction models for sensor time series[17]. But LSTM is few shown in recent GPS land deformation trend analysis papers. Moreover, most LSTM networks for land deformation trend prediction received unprocessed noisy raw data as input, which confuses the network with wrong prior

knowledge. Since Kalman filter has been proved to enhance LSTM networks' performance[18], it is natural for us to think about applying LSTM networks with unified trend extraction model as preprocessed step.

This paper studies the feasibility and practical implementation of an unified comprehensive framework that can satisfy both land deformation trend extraction and prediction from low cost GPS sensors. We model slowly moving displacement [2] as variations of mean level in daily measurements, and treat collected time series as samples from the distribution of each measurement. In this case, all of the discontinuity within a day can be avoided. Then, by refining state space method defined as Dynamic Linear Model (DLM) proposed in[19], and combining it with LSTM networks, we develop an end-to-end DLM-LSTM framework to solve trend analysis in discontinuous low cost GPS sensor time series. The major contribution of our framework lies as follows:

1. The introduced DLM model expands both the observation matrix and evolution matrix of state space function to contain harmonic operators for periodical variation modeling and first order AR operators for autocorrelation in residuals. These expansions allow DLM to extract displacement trend with higher precision from noisy, discontinuous, periodically variable, and autoregressive low cost GPS time series.
2. For sequence prediction, the introduced LSTM networks receive training preprocessed samples. Those training samples provide validated prior knowledge of land deformation trends, which enhances LSTM networks' power in both linear and non-linear time series prediction. LSTM networks will receive lower mean square error, which means that prediction sequence will be in more closer to real land deformation trends.
3. The fusion of DLM and LSTM provides an end-to-end north-south land deformation trend analysis workflow, which can do both trend extraction and prediction jobs. Our framework is able to model discontinuous low cost GPS time series without other operations. The raw sensor data received by wireless sensor networks can be used as input directly.

To test our DLM-LSTM framework, spatial-temporal distributed low cost latitude time series (LCLTS) dataset is constructed using deployed wireless GPS sensors on both the moving southern slope of the Fushun Western Open-pit Coal Mine (FWOCM) and static comparative field in Baoxie, Wuhan, China. All GPS sensors that provide latitude time series are in the same type. Experiments have shown that our framework extracts and predicts submeter level north-south deformation in FWOCM from February to March in 2017, which coincides with manual measurement at same point. Also, trend extracted in Baoxie field from November to December, 2016, remains to be static at submeter level. The two results validate our framework and prove its time and space independence.Like [20], our sensor network complements InSAR in high resolution north-south deformation detection. Steady observations reveal local features of 2-dimensional mine surface motion, which are valuable resources for researchers and authorities.

The paper is organized as follows. In Section 2, the DLM-LSTM framework is presented. The processing results on LCLTS dataset are shown in Section 3. The conclusion is given in Section 4.

2. DLM-LSTM Framework for Deformation Trend Extraction and Forecast

2.1. Description of DLM-LSTM Framework

By analyzing the characteristics of latitude time series and comparing it with field observations, the land deformation shows a stepwise character, which means obvious mean latitude level changing can be observed between adjacent days, but latitude within each day remains stationary. Also, long term measurement implies that land displacement contain periodic components, which triggers the fluctuations that mask the monotonic trends. Hence, the proposed method filter these disturbances to obtain monotonic deformation trends. Figure1 shows the flow chart of our DLM-LSTM framework. Firstly, the latitudes received every day are modeled as samples from a Gaussian distributions.

Mean level and standard deviation are calculated as the observed variables to state space equations of Dynamic Linear model. Then the states in the DLM model equations are predicted using recursive Kalman Filter formula. Finally the land deformation trend is extracted by recursive Kalman Smoother. We apply a simulation smoother in the last step of DLM to describe the full joint distribution of all states and the characteristic of extracted trends. After DLM finished its job, the deformation trend is transferred to LSTM networks for training. When network parameters are estimated, LSTM networks are able to predict the displacement using prior trend knowledge. In the end , extracted and predicted deformation trend are compared with observed ground truth displacement to evaluate the performance of our framework.

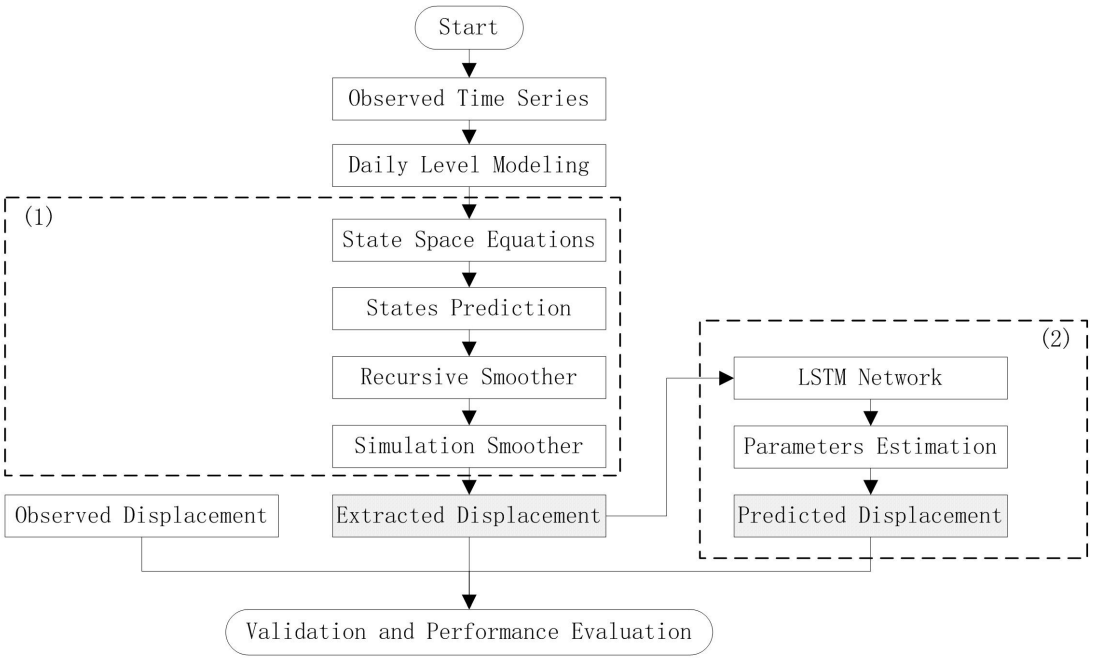

Figure 1. Flow chart of proposed DLM-LSTM framework. (**1**) Dynamic Linear Model using recursive Kalman formula for parameter estimation. (**2**) Recurrent LSTM networks.

2.2. Dynamic Linear Model

Dynamic Linear Model was first defined and introduced in analyzing trends in stratosphere ozone time series[19]. From the definition, "dynamic" was explained as evolution of regression coefficient in time and "linear" means the state space equations are all linear. From my understanding, DLM is the general form of Kalman Filter functions. By adding additional operators to the observation matrix and evolution matrix, simple Kalman Filter can denoise complex time-varying time series to obtain validated trends. In the following subsections, we will introduce the state space function of DLM designed for low cost GPS time series and Kalman recursive method for parameters estimation. The land deformation trend will be extracted after the parameters are fully estimated.

2.2.1. State Space Functions

The general Kalman State Space Model is written as:

$$\mathbf{y}_t = \mathbf{F}_t \mathbf{x}_t + \mathbf{v}_t \qquad \mathbf{v}_t \sim \mathbf{N}(0, \mathbf{V}_t) \tag{1}$$

$$\mathbf{x}_t = \mathbf{G}_t \mathbf{x}_{t-1} + \mathbf{w}_t \qquad \mathbf{w}_t \sim \mathbf{N}(0, \mathbf{W}_t) \tag{2}$$

where $\mathbf{y}_t$ are the observations at time t, $t = 1, ..., n$. The unobserved states, in our case the deformation trends, are defined as vector $\mathbf{x}_t$, which evolves in time with noise $\mathbf{w}_t$ according to evolution matrix $\mathbf{G}_t$ in equation (2). The relationship between observed and unobserved states are described in observation equation (1), where result of $\mathbf{x}_t$ transformed by observation matrix $\mathbf{F}_t$ combining noise v_t leads to $\mathbf{y}_t$. Both noises w_t and v_t lies in Gaussian distribution with covariance $\mathbf{W}_t$ and $\mathbf{V}_t$.

DLM model first expand vectors in equation (1) and (2) in the following form:

$$\begin{gathered} \mathbf{x}_t = \left[u_t, \alpha_t\right]^T, \qquad \mathbf{G}_{trend} = \begin{bmatrix} 1 & 1 \\ 0 & 1 \end{bmatrix}, \qquad \mathbf{F}_{trend} = \left[1, 0\right], \\ \mathbf{W}_{trend} = \begin{bmatrix} \sigma^2_{level} & 0 \\ 0 & \sigma^2_{trend} \end{bmatrix}, \qquad \mathbf{V}_t = \left[\sigma_{obs(t)}\right] \end{gathered} \tag{3}$$

where u_t is the mean level of latitude each day and α_t is the change in the level from day t to day $t+1$. Correspondingly, $\mathbf{W}_t$ is decomposed to two components: the Gaussian noise distribution with standard deviation σ_{level} and σ_{trend}. This form of DLM model is able to detect smooth varying in the mean level and infer changes happened in land surface, but it does not consider periodic fluctuations.

To detect periodic fluctuations, DLM models them using harmonic functions. The corresponding operators in observation matrix is defined as:

$$\begin{gathered} \mathbf{G}_{peri(k)} = \begin{bmatrix} \cos\left(k2\pi/30\right) & \sin\left(k2\pi/30\right) \\ -\sin\left(k2\pi/30\right) & \cos\left(k2\pi/30\right) \end{bmatrix} \\ \mathbf{F}_{peri} = \left[1, 0\right], \qquad \mathbf{W}_{peri} = \begin{bmatrix} \sigma^2_{peri(k)} & 0 \\ 0 & \sigma^2_{peri(k)} \end{bmatrix} \end{gathered} \tag{4}$$

where k means the k_{th} harmony detected in daily level series within 30 days. We adjust number k to reach the best performance during the experiment.

Because paper [16] reveals autoregressive characteristic in the time series of slowly moving surface displacement, we use a first-order autoregressive model for residual components, $\eta_t = \rho\eta_{t-1} + \epsilon_{AR}$, with $\epsilon_{AR} \sim N\left(0, \sigma_{AR}\right)$. In DLM form, we have:

$$\mathbf{G}_{AR} = \left[\rho\right], \qquad \mathbf{F}_{AR} = \left[1\right], \qquad \mathbf{W}_{AR} = \left[\sigma^2_{AR}\right] \tag{5}$$

To extract land deformation trend from daily latitude time series, the DLM model must combine all the operators above, which leads to larger scale evolution and observation matrix as below:

$$\begin{gathered} \mathbf{G} = \begin{bmatrix} \mathbf{G}_{trend} & 0 & 0 & 0 \\ 0 & \mathbf{G}_{peri(5)} & 0 & 0 \\ 0 & 0 & \mathbf{G}_{peri(10)} & 0 \\ 0 & 0 & 0 & \mathbf{G}_{AR} \end{bmatrix} \\ \mathbf{F}_t = \begin{bmatrix} \mathbf{F}_{trend} & \mathbf{F}_{peri(5)} & \mathbf{F}_{peri(10)} & \mathbf{F}_{AR} \end{bmatrix} \end{gathered} \tag{6}$$

where $\mathbf{G}_{peri(5)}$ and $\mathbf{G}_{peri(10)}$ are the 5_{th} and 10_{th} harmonies of 30 days circulation. These two harmonies are found to outperform other combination in periodic variations denoise. Other operators remain the same as above. Respectively, we have state vector $\mathbf{x}_t$ as belows:

$$\mathbf{x}_t = \begin{bmatrix} \mu_t & \alpha_t & u_{peri(5)} & u^*_{peri(5)} & u_{peri(10)} & u^*_{peri(10)} & \eta_t \end{bmatrix}^T \tag{7}$$

These DLM state space equations contain unknown parameters, including covariance matrix $\mathbf{V}_t$, AR coefficient ρ and etc. In the following step, these parameters will be fully estimated to put DLM into real applications.

2.2.2. Model Parameters Estimation

In DLM, the unknowns are divided into two major categories: model state $\mathbf{x}_t$ and auxiliary parameters defined in state space equations. In this paper, we select Falman formula method proposed in paper [19] to obtain the unknown trends and parameters. The essence of Kalman formula is the recursive prediction and comparison. By continuously updating the covariance matrix in the state space equations, Kalman formula construct the connections between measurement and hidden real states. Firstly, we perform Kalman filter forward recursion to predict states $\mathbf{x}_t$, we assume the conditional probability of predicted states $\mathbf{x}_{t+1}$ follow normal distributions as below:

$$p\left(\mathbf{x}_{t+1}|\mathbf{x}_t, \mathbf{y}_{1:t}, \boldsymbol{\theta}\right) = N\left(\widehat{\mathbf{x}}_{t+1}, \widehat{\mathbf{C}}_{t+1}\right) \tag{8}$$

where $\boldsymbol{\theta}$ represents all the unknown parameters in vector form. Based on this assumption, the daily latitude mean level and standard deviation can be applied as input prior knowledge.Then, Kalman filter is used as below:

$$\mathbf{v}_t = \mathbf{y}_t - \mathbf{F}_t\mathbf{G}_t\overline{\mathbf{x}}_{t-1} \qquad prediction \quad residual \tag{9}$$

$$\widehat{\mathbf{C}}_t = \mathbf{G}_t\overline{\mathbf{C}}_{t-1}\mathbf{G}_t^T + \mathbf{W}_t \qquad prior \quad covariance \quad for \quad x_t \tag{10}$$

$$\mathbf{C}_t^y = \mathbf{F}_t\widehat{\mathbf{C}}_t\mathbf{F}_t^T + \mathbf{V}_t \qquad covariance \quad for \quad prediction \quad y_t \tag{11}$$

$$\mathbf{K}_t = \widehat{\mathbf{C}}_t\mathbf{F}_t^T\left(\mathbf{C}_t^y\right)^{-1} \qquad Kalman \quad gain \tag{12}$$

$$\overline{\mathbf{x}}_t = \mathbf{G}_t\overline{\mathbf{x}}_{t-1} + \mathbf{K}_t\mathbf{v}_t \qquad next \quad state \quad prior \quad mean \tag{13}$$

$$\overline{\mathbf{C}}_t = \widehat{\mathbf{C}}_t - \mathbf{K}_t\mathbf{F}_t\widehat{\mathbf{C}}_t \qquad next \quad state \quad prior \quad covariance \tag{14}$$

Then, we apply Kalman smoother backward to get the smoothed land deformation trend:

$$\mathbf{L}_t = \mathbf{G}_t - \mathbf{G}_t\mathbf{K}_t\mathbf{F}_t \tag{15}$$

$$\mathbf{r}_t = \mathbf{F}_t^T\left(\mathbf{C}_t^y\right)^{-1}\mathbf{v}_t + \mathbf{L}_t^T\mathbf{r}_{t+1} \tag{16}$$

$$\mathbf{N}_t = \mathbf{F}_t^T\left(C_t^y\right)^{-1}\mathbf{F}_t + \mathbf{L}_t^T\mathbf{N}_{t+1}\mathbf{L}_t \tag{17}$$

$$\widetilde{\mathbf{x}}_t = \mathbf{G}_t\overline{\mathbf{x}}_{t-1} + \widehat{\mathbf{C}}_t\mathbf{r}_t \qquad smoothed \quad latitude \quad trend \tag{18}$$

$$\widetilde{\mathbf{C}}_t = \widehat{\mathbf{C}}_t - \widehat{\mathbf{C}}_t\mathbf{N}_t\widehat{\mathbf{C}}_t \qquad smoothed \quad state \quad covariance \tag{19}$$

2.3. LSTM Recurrent Networks

Time series prediction is about taking some previous input terms, putting them through some hidden units, and predicting the next term. In the past, computer scientists favorite Hidden Markov Model (HMM). As the sequence grows larger and larger, the bits of information HMM need to remember explode. Therefore, recurrent neural networks (RNN) is developed to substitute HMM by storing more prior knowledge in distributed way. With several different input remembered at once, RNN is able to predict more complicated dynamics.

In our paper, we developed an LSTM RNN for land deformation trend prediction. LSTM, so called long-short time memory units, is a special type of RNN neural. As Figure2 shows, in each LSTM units, three gates are designed. The gates serve to help LSTM interacts between the memory cell itself and its environment. The input gate can allow incoming signal to update the state of the memory cell or block it. On the other end, the output gate can allow the state of the memory cell to have an effect on other neurons or prevent it. Finally, the forget gate can modulate the memory cell's self-recurrent connection, allowing the cell to remember or forget its previous state, as needed. The whole network contains four LSTM memory cells. After time sequence passes these units, the outputs will be pooled by a mean pooling units to get the predicted value.

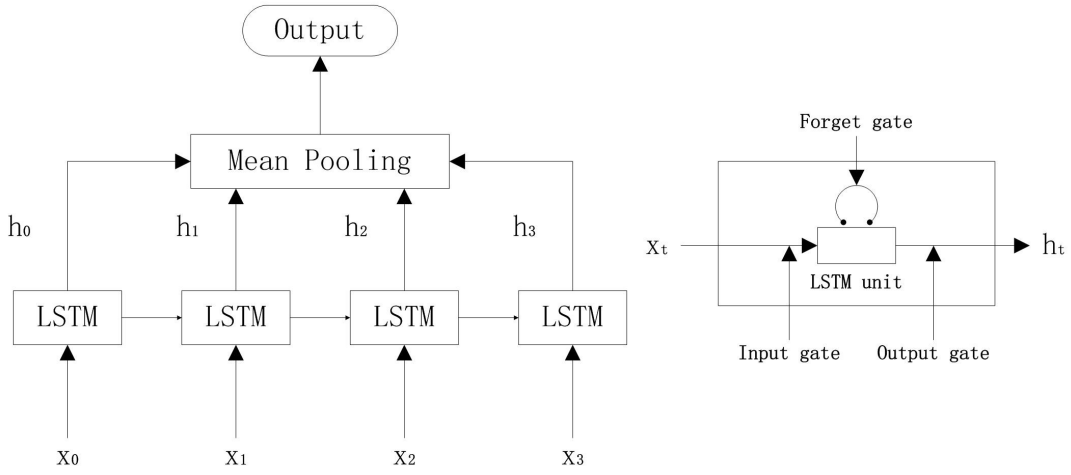

Figure 2. Applied LSTM recurrent network. **left**: Network structure **right**: LSTM unit structure.

3. Case Studies

With the aim to illustrate the effectiveness of the DLM-LSTM framework proposed, one land surface deformation cases and one static case are studied in the following subsections.

3.1. Case 1: Fushun Western Open-pit Coal Mine

3.1.1. Dataset

Coal mining in the FWOCM started in the early twentieth century. Production of coal used to be a pillar of the Fushun economy. Decades of mining techniques are causing frequent surface deformation and landslides that threaten the city, Fushun. As Figure3 shows, an open pit with a length of *6600 m* east-to-west and width of *2200 m* north-to-south stands among the residential districts [21], [22]. Therefore, landslides represent a serious threat to miners and local people. According to our field investigation, deformation in the north-south direction is more worse than in the east-west direction. A fault zone was spotted between conveyor belts that transport coal to the surface and residential buildings. To protect the buildings and peoples nearby, we deployed the WSN on the south slope near the conveyer belt.

Figure 3. The WSN position on the southern slope of FWOCM.

An inexpensive system including hardware and software, was designed for monitoring the surface displacement of the southern slope of the FWOCM. The system consists of two parts, a WSN and a remote server. The sensor nodes of the WSN transmit the data to the remote server as soon as they are received. The data are stored, processed and published on the web in the server. No processing is running on the sensor nodes due to the lack of electricity in the field.

The WSN with a star topology was composed of two kinds of nodes, sensor nodes and a coordinator. All the sensor nodes send their data to the coordinator, and the coordinator forwards the data to the server through a connected General Packet Radio Service (GPRS) module. Both the sensor node and the coordinator were developed using CC2530 ZigBee development board. For sensor nodes, sensor was connected to the board through peripherals, such as GPIO or UART. The sensors were a 3-dimensional digital compass (DCM308), GPS (Ublox NEO-6M) and low cost Inertial Measurement Unit (IMU), soil humidity, soil temperature, atmospheric pressure, atmospheric temperature, atmospheric humidity, and a rain gauge. The communication protocol for data transmission between multiple sensor nodes and coordinators was developed based on Z-stack (TI's API for low-cost ZigBee communication). The protocol adapts to the Solar powered network. The sensor node can find the coordinator and establish a communication link automatically. Figure 3 shows the position of the WSN. The WSN has been working well since Dec. 1, 2014.

Figure4 shows the layout of three GPS+IMU sensor nodes. The three nodes were located near $N41°50'$, $E123°52'$. A GPS sensors were positioned in a line on the north side, while the other one was placed on the south side. The horizontal position accuracy of the GPS receiver (L1 frequency, C/A code) is $2.5\ m$. As the sensor data accumulate, long term land motion calculations based on current and historical data become practical and feasible. In our paper we select the north side GPS sensor as our data source, and collect latitude data from February 1st to March 2nd in 2016. The latitudes are numbered according to the interval between the date of the latitude and February 1st, which means the latitudes in March 1st are numbered as day 30.

Figure 4. Layout of GPS+IMU sensor nodes in FWOCM.

Figure5 shows the latitude samples collected each day. As shown in the figure, there is a significant continuity in latitude time series. The latitudes from February 1st to February 6th are all missed, while latitudes from February 6th to February 20th lacks in quantity. Based on these situation, our DLM-LSTM framework will be proved effective if it is able to extract land deformation trend in sub-meter accuracy.

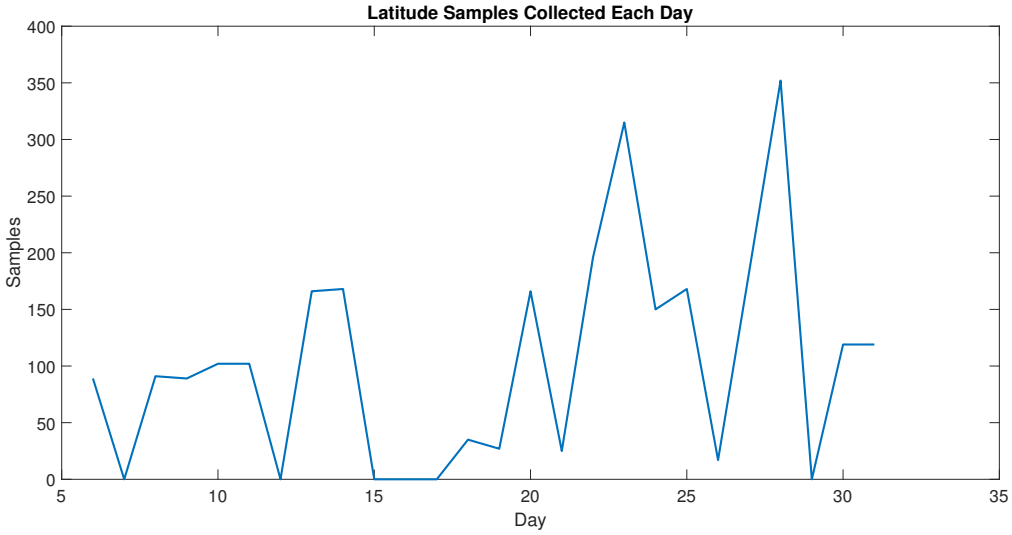

Figure 5. Latitude samples between February 1st and March 2nd in 2016

3.1.2. Results

We first calculated the mean level and standard deviation in each day to form latitude level time series. Then we chose time series from Day 6 to Day 31 as the input to our DLM model. Figure6 shows the result of DLM model in land deformation trend extraction. As shown in the Figure6, DLM constructs an estimated trend from discontinuous mean latitude points and gives the 95% probability envelope. Figure7 shows the result of diagnostic analysis on the residuals by plotting estimated autocorrelation function and normal probability. In the ACF line, dashed horizontal lines represent the approximative region where the coefficient do not significantly from deviate from zero.

228 Figure6 and Figure7 validate extracted trend in statistical way. After latitude degrees are transferred
229 to minimeters, we are able to compare the extracted displacement with ground truth.

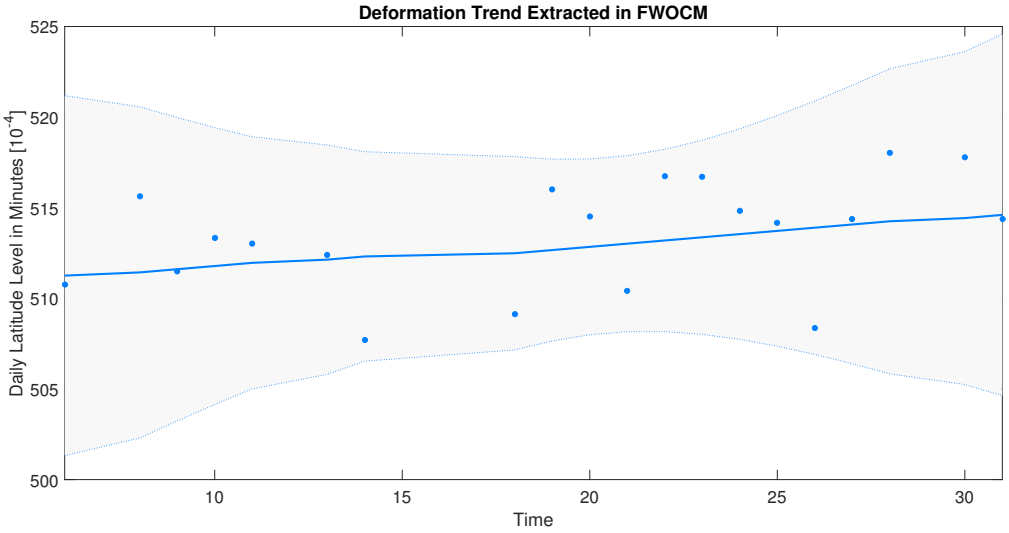

Figure 6. The result of deformation trend extraction

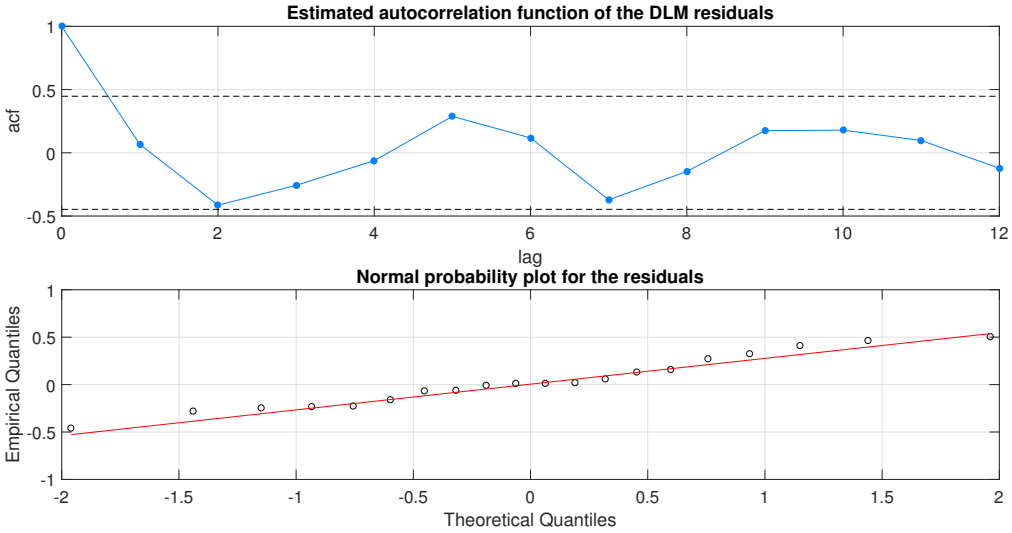

Figure 7. Analysis of the DLM residuals

230 Figure8 shows the comparison of the extracted deformation trend with the ground truth. The
231 ground truth comes from manual measurement on daily displacement in the same period. From the
232 Figure8, we can see that our extracted trend shows a centimeter level consistency with the manual
233 measurement. The result of DLM's performance is given in Table 1 by RMSE, MAPE, R^2, and PA.

Table 1. Performance of DLM Model

RMSE(mm)	**MAPE**	R^2	**PA(%)**
17.21292774	0.09301	0.990329206	9.3

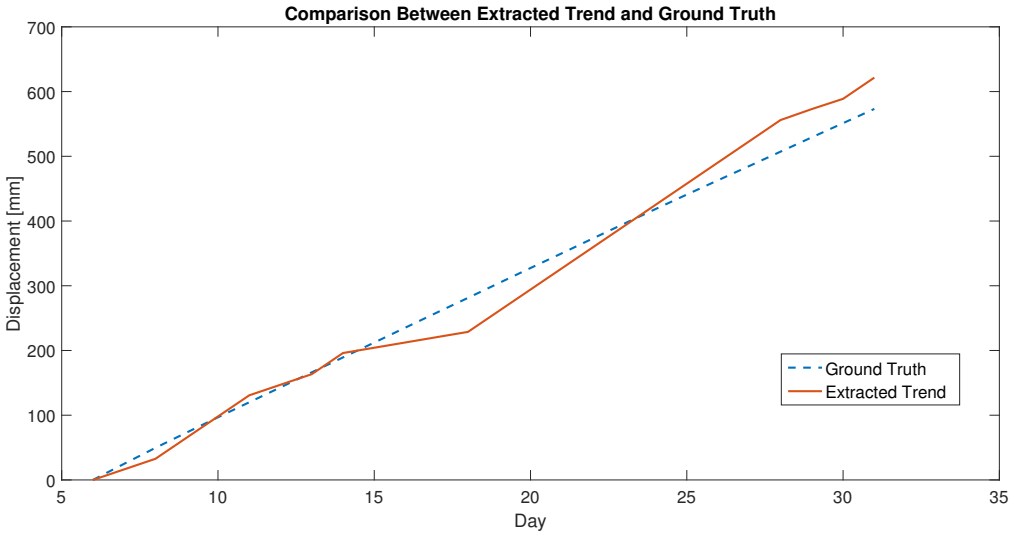

Figure 8. Comparison of the extracted deformation trend with the mannual measurement displacement

Obviously, results in Table 1 indicates that the extraction performance of DLM is surprising. The error between extracted trend and ground truth remains at centimeter level. As our GPS latitude sensors have 2.5m navigation error, these result is a big step in accuracy improvement. Therefore, DLM is proved to be effective in trend extraction from noisy discontinuous low cost GPS sensors.

As the DLM's performance is validated, the trend can be used as input to our 4 unit LSTM networks. We select trend from Day 1 to Day 26 as our training samples and try to predict the following 13 days' trend. The network parameters are shown in Table 2. Figure9 shows the comparison result of our prediction and ground truth measurement. Our LSTM network predict 13 days' deformation trend with 22.1722mm RMSE in Table 3, which proves that LSTM network also has accuracy improvement effect in trend prediction. Although prediction trend deviate ground truth line since Day 32, its sub-meter level result can still be validated. Future works may pay attention on improving LSTM network's performance.

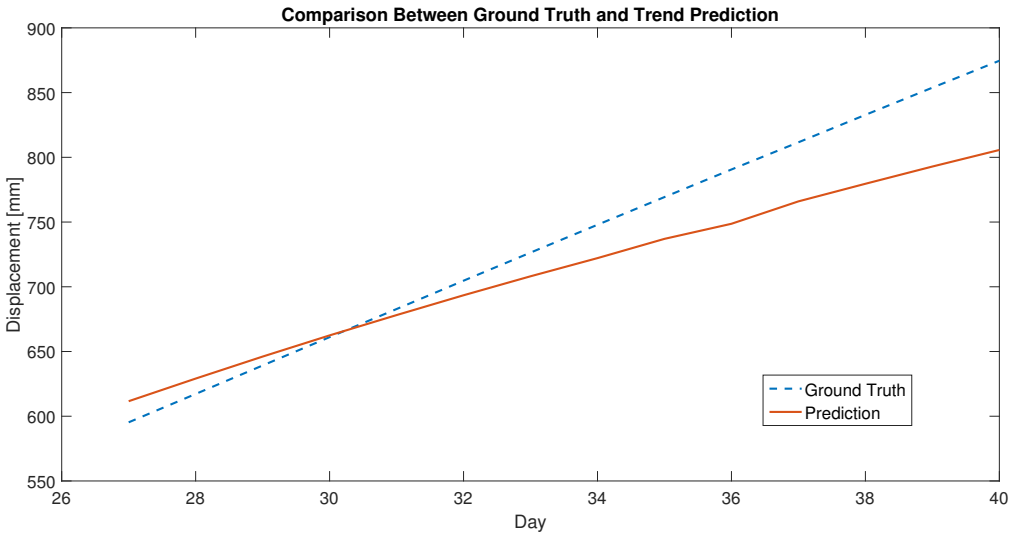

Figure 9. Displacement prediction by LTSM

Table 2. Parameters of LSTM Networks

Loss Function	Optimizer	Batch Size	Epoch)
Mean Square Error	SGD	3	1500

Table 3. Performance of LSTM Networks

RMSE(mm)	MAPE	R^2	PA(%)
22.17225596	0.03622	0.939247	9.4

3.2. Case 2: Baoxie Sensor Web Experimental Field

3.2.1. Dataset

To prove that our DLM has locational invariant propriety, we need to find another place to conduct validation experiment. Baoxie Sensor Web Experiment Field, located in the east of Wuhan central area, is the main Sensor Web research and experiment place for Wuhan University's State Key Laboratory for Information Engineering in Surveying, Mapping and Remote Sensing (LIESMARS). It contains four stations: Baoxie Landslide Monitoring Station, Baoxie Meteorological Experimental Station, Baoxie Edaphic and Meteorological Monitoring Station, and Baoxie Soil Temperature and Moisture Monitoring Station. These stations, in total, are about $800m^2$ with more than 70 sensors.All of the sensors are powered by photovoltaic solar energy. Previously, LIESMARS successfully built a Cyber-Physical Geographical Information paradigm for In-situ Land surface Monitoring[23], which provided solid basis for our experiment. As Figure10 implies, we select a GPS sensor in a wireless sensor node deployed since 2013 as our experimental data source.The position of this GPS sensor is $N30°28'$, $E114°31'$. The horizontal position accuracy of the GPS receiver (L1 frequency, C/A code) is the same as FWOCM, which is *2.5 m*.

Figure 10. Baoxie Meteorological Experimental Station

We collected 14 days' latitude data from December 1st to December 14. Figure11 shows the latitude samples received each day. It is obvious to find that GPS sensor in Baoxie works more stable than FWOCM, which has larger deviation in sample numbers each day. But still, Baoxie sensor suffers discontinuity, which is same as FWOCM. Also, In-situ station measurement shows that location $N30°28'$, $E114°31'$ remains static with no centimeter level deformation in the same period, which provides the ground truth.

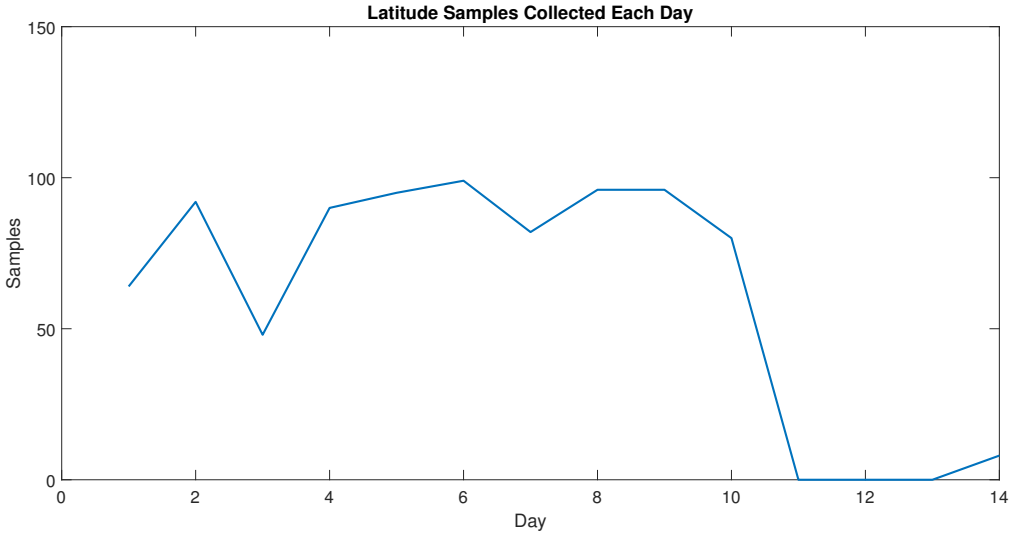

Figure 11. Latitude sampls at Baoxie, Wuhan, China

3.2.2. Results

Figure12, Figure13 show the extracted trend and residual analysis of GPS sensor from Baoxie Sensor Web Experimental Field. From Figure12 and Figure13, we can see that an obvious static trend is obtained by DLM. For further statistical test, because the ground truth is recognized as zero, only RMSE can be calculated in Baoxie. The RMSE is 2.354mm, which obviously prove DLM's capability in extracting trend from low cost GPS sensors.

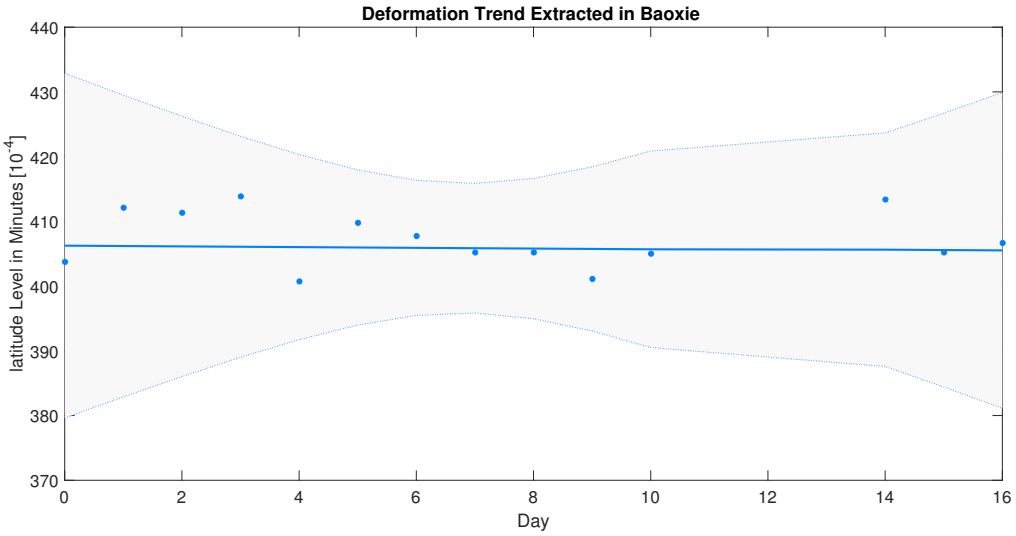

Figure 12. Trend extraction by DLM at Baoxie

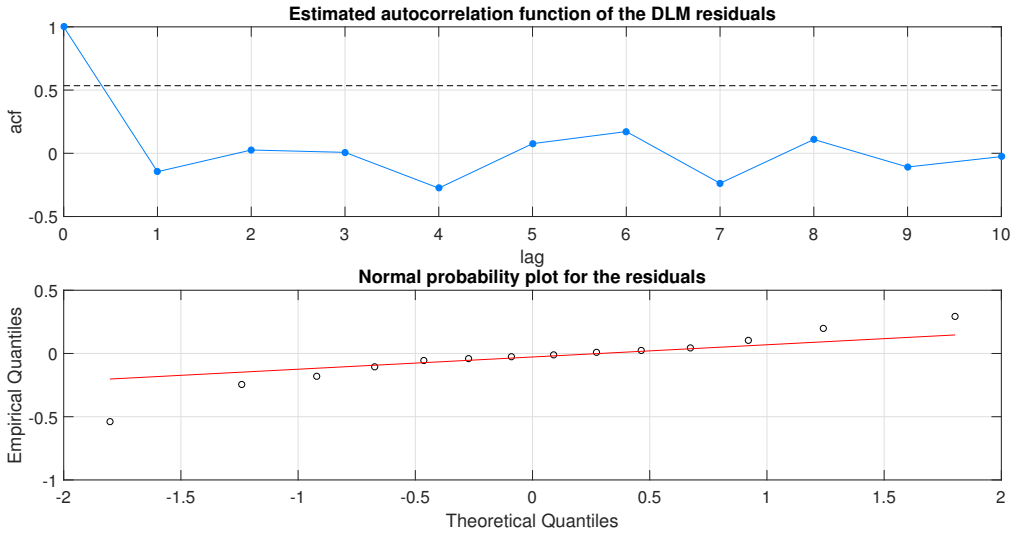

Figure 13. Residual analysis by DLM at Baoxie

4. Conclusions

A DLM-LSTM framework was proposed and applied for north-south deformation trend analysis from low cost GPS time series. Dynamic Linear Model was first introduced to model the relation of measurement with state vector that includes mean level trend, noise, periodic variation and autoregressive component hidden in latitude sequence. Then land deformation trend is extracted utilizing recursive Kalman filter and smoother. LSTM recurrent neural networks is introduced to predict the next states in deformation trend. By analyzing two land deformation cases, the performance of proposed method was evaluated quantitatively. Calculated displacement in extracted trend from DLM is excellently consistent with manual measurement from the latitude series of FWOCM. The centimeter level accuracy was first obtained in north-south deformation trend, which is difficult to obtain by satellite remote sensing approaches. Meanwhile, centimeter level accuracy is also achieved in trend prediction by LSTM networks. Results of this work indicate that DLM-LSTM framework is a powerful and accurate end-to-end method to analyze land surface deformation trend.

Acknowledgments: This work was supported by the National Key Research and Development Program of China under Grant No. 2016YFB0502601. It was aslo supported by the Fundamental Research Funds for the Central Universities under Grant no.2042017kf0211.

Author Contributions: Prof. Pu contributed to the framework. Mr. Xu conveived and designed the experiments. Prof. Chen and Prof. Gong directed the establishement of WSN and the analysis of the data.

Conflicts of Interest: The authors declare no conflict of interest.The founding sponsors had no role in the design of the study; in the collection, analyses, or interpretation of data; in the writing of the manuscript, and in the decision to publish the results.

Abbreviations

The following abbreviations are used in this manuscript:

GPS	Globe positioning systems
SAR	Synthetic aperture radar
DInSAR	Differential interferometric synthetic aperture radar
ICT	Information Communication Technology
RTK	Real-Time Kinematic
UAV	Unmanned aerial vehicles
C/A	Coarse Acquisition
LD	linear dichroism

Bibliography

1. Petley, D. Global patterns of loss of life from landslides. *Geology* **2012**, *40*, 927–930.
2. Thiebes, B. *Landslide Analysis and Early Warning Systems: Local and Regional Case Study in the Swabian Alb, Germany*; Springer Science & Business Media, 2012.
3. Zheng, D.; Frost, J.; Huang, R.; Liu, F. Failure process and modes of rockfall induced by underground mining: A case study of Kaiyang Phosphorite Mine rockfalls. *Engineering Geology* **2015**, *197*, 145 – 157.
4. Hilley, G.E.; Bürgmann, R.; Ferretti, A.; Novali, F.; Rocca, F. Dynamics of Slow-Moving Landslides from Permanent Scatterer Analysis. *Science* **2004**, *304*, 1952–1955.
5. Macciotta, R.; Hendry, M.; Martin, C.D. Developing an early warning system for a very slow landslide based on displacement monitoring. *Natural Hazards* **2016**, *81*, 887–907.
6. Strozzi, T.; Farina, P.; Corsini, A.; Ambrosi, C.; Thüring, M.; Zilger, J.; Wiesmann, A.; Wegmüller, U.; Werner, C. Survey and monitoring of landslide displacements by means of L-band satellite SAR interferometry. *Landslides* **2005**, *2*, 193–201.
7. Akbarimehr, M.; Motagh, M.; Haghshenas-Haghighi, M. Slope Stability Assessment of the Sarcheshmeh Landslide, Northeast Iran, Investigated Using InSAR and GPS Observations. *Remote Sensing* **2013**, *5*, 3681–3700.
8. Tofani, V.; Raspini, F.; Catani, F.; Casagli, N. Persistent Scatterer Interferometry (PSI) Technique for Landslide Characterization and Monitoring. *Remote Sensing* **2013**, *5*, 1045–1065.
9. Raspini, F.; Cigna, F.; Moretti, S. Multi-temporal mapping of land subsidence at basin scale exploiting Persistent Scatterer Interferometry: case study of Gioia Tauro plain (Italy). *Journal of Maps* **2012**, *8*, 514–524.
10. He, L.; Wu, L.; Liu, S.; Wang, Z.; Su, C.; Liu, S.N. Mapping Two-Dimensional Deformation Field Time-Series of Large Slope by Coupling DInSAR-SBAS with MAI-SBAS. *Remote Sensing* **2015**, *7*, 12440–12458.
11. Bae, T.S.; Grejner-Brzezinska, D.; Mader, G.; Dennis, M. Robust Analysis of Network-Based Real-Time Kinematic for GNSS-Derived Heights. *Sensors* **2015**, *15*, 27215–27229.
12. Jo, H.; Sim, S.H.; Tatkowski, A.; Spencer, B.; Nelson, M.E. Feasibility of displacement monitoring using low-cost GPS receivers. *Structural Control and Health Monitoring* **2013**, *20*, 1240–1254.
13. Gomez-Gil, J.; Ruiz-Gonzalez, R.; Alonso-Garcia, S.; Gomez-Gil, F.J. A kalman filter implementation for precision improvement in low-cost GPS positioning of tractors. *Sensors* **2013**, *13*, 15307–15323.
14. Gao, J.x.; Hong, H.; Fei, L.; Li, Z.k.; Yao, Y.f. Signal extraction for GPS deformation monitoring in mining survey. *Transactions of Nonferrous Metals Society of China* **2014**, *24*, 3949–3954.
15. Zhang, J.; Peng, W.; Liu, F.; Zhang, H.; Li, Z. Monitoring Rock Failure Processes Using the Hilbert–Huang Transform of Acoustic Emission Signals. *Rock Mechanics and Rock Engineering* **2016**, *49*, 427–442.
16. Pu, F.; Ma, J.; Zeng, D.; Xu, X.; Chen, N. Early Warning of Abrupt Displacement Change at the Yemaomian Landslide of the Three Gorge Region, China. *Natural Hazards Review* **2015**, *16*.
17. Lipton, Z.C.; Kale, D.C.; Elkan, C.; Wetzell, R. LEARNING TO DIAGNOSE WITH LSTM RECURRENT NEURAL NETWORKS **2015**.
18. Perezortiz, J.A.; Gers, F.A.; Eck, D.; Schmidhuber, J. Kalman filters improve LSTM network performance in problems unsolvable by traditional recurrent nets. *Neural Networks* **2003**, *16*, 241–250.
19. Laine, M.; Latvapukkila, N.; Kyrola, E. Analysing time-varying trends in stratospheric ozone time series using the state space approach. *Atmospheric Chemistry and Physics* **2014**, *14*, 9707–9725.
20. Li, X.; Liu, Q.; Yang, R.; Wen, J.; Zhang, J.; Cai, E.; Zhang, H. The Combination of Ground-Sensing Network and Satellite Remote Sensing in Huailai County. *IEEE Sensors Journal* **2016**, *16*, 3819–3826.
21. Nie, L.; Li, Z.; Zhang, M.; Xu, L. Deformation characteristics and mechanism of the landslide in West Open-Pit Mine, Fushun, China. *Arabian Journal of Geosciences* **2015**, *8*, 4457–4468.
22. Johnson, E.A. Geology of the Fushun coalfield, Liaoning province, People's Republic of China. *International Journal of Coal Geology* **1990**, *14*, 217–236.
23. Chen, N.; Xiao, C.; Pu, F.; Wang, X.; Wang, C.; Wang, Z.; Gong, J. Cyber-Physical Geographical Information Service-Enabled Control of Diverse In-Situ Sensors. *Sensors* **2015**, *15*, 2565–2592.

Sample Availability: Samples of the compounds ..... are available from the authors.